

Gold Sputtered Fiducial Markers for Combined Secondary Ion Mass Spectrometry and MALDI Imaging of Tissue Samples

Nina Ogrinc Potočnik,^{†,‡,⊥} Karolina Škrášková,^{||,#,⊥} Bryn Flinders,[#] Primož Pelicon,[†] and Ron M. A. Heeren^{*,#}

[†]Jozef Stefan Institute, Jamova 39, SI-1000 Ljubljana, Slovenia

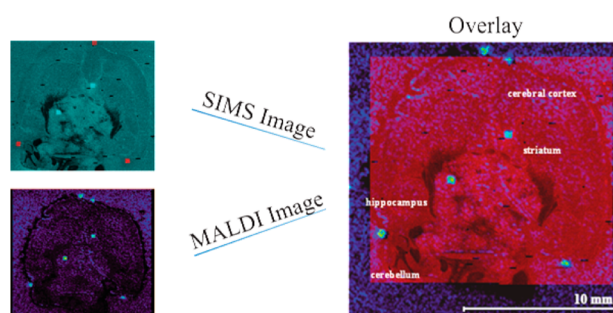
[‡]LOTRIČ ltd, Selca 163, SI-4227 Selca, Slovenia

^{||}Charles University in Prague, Faculty of Pharmacy, Heyrovského 1203, 500 05 Hradec Králové, Czech Republic

[#]FOM Institute AMOLF, Science Park 104, 1098 XG Amsterdam, The Netherlands

S Supporting Information

ABSTRACT: Mass spectrometry imaging (MSI) is a label free technique capable of providing simultaneous identification and localization of biomolecules. A multimodal approach is required that allows for the study of the complexity of biological tissue samples to overcome the limitations of a single MSI technique. Secondary ion mass spectrometry (SIMS) allows for high spatial resolution imaging while matrix-assisted laser desorption ionization (MALDI) offers a significantly wider mass range. The combination of coregistered SIMS and MALDI images results in detailed and unique biomolecular information. In this Technical Note, we describe how gold sputtered/implanted fiducial markers (FM) are created and can be used to ensure a proper overlay and coregistration of the two-dimensional images



provided by the two MSI modalities.

Mass spectrometry imaging (MSI) is a label free technique which provides an insight into the elemental and molecular spatial distribution of complex sample surfaces. For this reason, it has been applied to a broad range of fields such as biology, biomedicine, pathology, and pharmacology.^{1,2} However, none of the available MSI techniques can individually provide the complete molecular information needed to study complex biological processes. Even though the three commonly used MSI techniques, secondary ion mass spectrometry (SIMS), matrix-assisted laser desorption ionization (MALDI), and desorption electrospray ionization (DESI), are under constant improvement, each of the techniques provides only limited information about the sample.^{2,3} SIMS for example has the capability of producing highly spatially resolved images of elements and smaller molecules but has a limited mass range. MALDI, on the contrary, has a better specificity and a broader mass range but lacks routine high spatial resolution imaging capabilities.^{4,5} The SIMS method is predominantly used for lipid investigation as a result of the substantial fragmentation produced by the primary ion beam.⁶ New primary ion sources such as Ar_n^+ and $(\text{H}_2\text{O})_n^{+7,8}$ beams reduce the fragmentation significantly and extend the application to larger biomolecules. MALDI is typically applied for the detection of larger biomolecules such as peptides and proteins and also offers a complementary perspective for lipid investigation. The combination of the two modalities can in part overcome their

individual limitations and provide broader insight into the different biomolecular distributions of tissue samples.^{9–13}

Biological tissue samples are very complex, and different tissues are presented to researchers in different forms.¹ Tissue sections without any distinctive anatomical features may cause a problem when trying to combine images acquired by different modalities.⁴ Tissue sections may also change their properties during measurements which inhibits correct alignment. In order to properly combine and coregister images from the two above-mentioned modalities (MALDI and SIMS), there is a need for specific fiducial markers (FM).¹⁴ FM have been widely used in magnetic resonance imaging (MRI),¹⁵ positron emission tomography (PET),¹⁶ and X-ray and therapeutic proton beam analysis,¹⁷ but they are usually inserted directly on the tissue section or inside an organ which changes the tissue integrity. Ink based FM have also been used for coregistration of different imaging modalities and further applied for a 3D reconstruction of an embedded human breast cancer xenograft.¹⁴

We have adopted a FM technique directly on rat brain and breast cancer (BC) tissue sections to allow for a direct correlation between the high resolution SIMS and MALDI images of the respective samples. The gold sputtered FM described in this paper were clearly observed by both

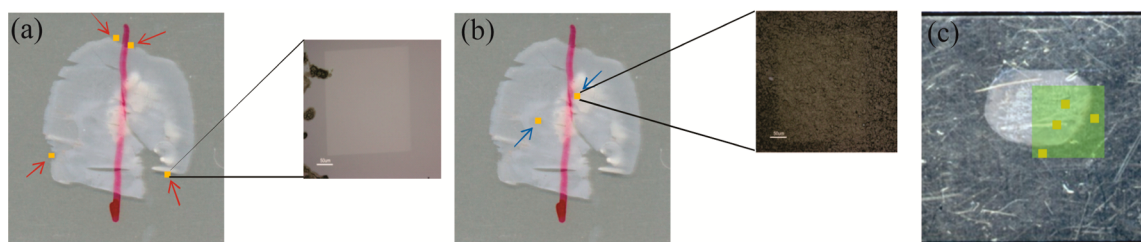


Figure 1. Optical images of 12 μm thick tissue sections and 500 $\mu\text{m} \times 500 \mu\text{m}$ gold sputtered FM are indicated by yellow squares. (a) Off-tissue FM adjacent to the brain tissue section (red arrows). (b) On-tissue FM on the brain tissue section (blue arrows). (c) Off- and on-tissue FM on the breast cancer tissue section. The large green square indicates the selected SIMS imaged region.

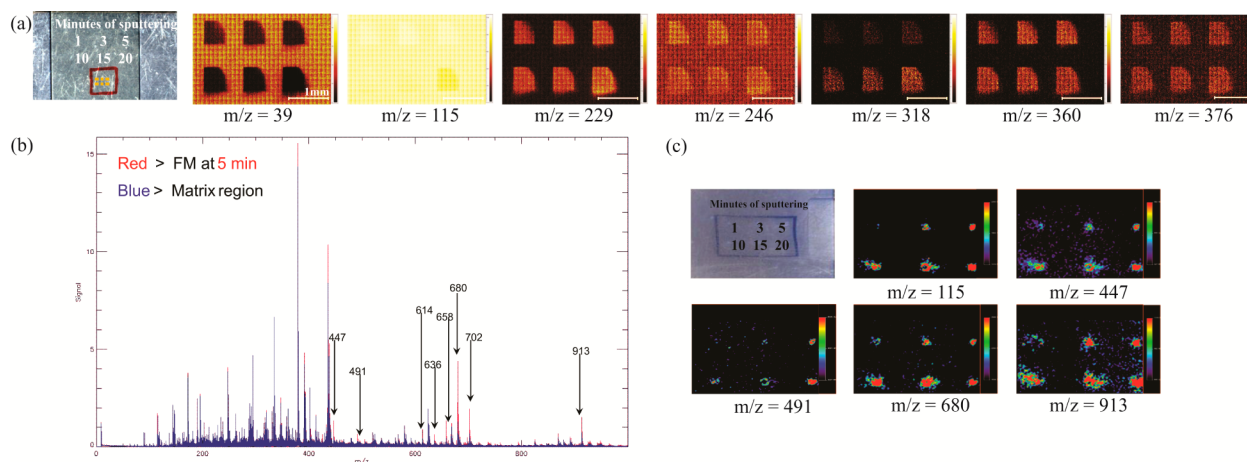


Figure 2. Blank ITO slide with sputtered FM. (a) High resolution SIMS images of FM at selected m/z values with sputtering times of 1, 3, 5, 10, 15, and 20 min. (b) Comparison of MALDI spectra of region of interest within the 5 min sputtered FM and the matrix region. (c) MALDI images of selected m/z values of the most abundant FM-related peaks with sputtering times of 1, 3, 5, 10, 15, and 20 min.

modalities. These new FM are advantageous over other ablation and marker techniques as a result of the known exact dimensions and the well-defined shape of the sputtered FM. They are therefore extremely suitable for subsequent coregistration of individual SIMS and MALDI measurements.

EXPERIMENTAL SECTION

Sample Preparation. Brain tissue of a healthy control rat and BC tissue of a patient-derived xenograft of a triple-negative breast cancer tumor were employed in the experiments. The 12 μm tissue sections were prepared with a cryo-microtome (HMS25, MICROM, Germany), thaw-mounted on the indium tin oxide (ITO) glass slides (Delta Technologies, USA), and stored at -80°C until further analysis. The sections were placed into a vacuum desiccator to avoid water condensation on the tissue surface prior to the actual MS measurements.

Fiducial Markers. The FM were created by sputtering a selected area of 500 $\mu\text{m} \times 500 \mu\text{m}$ on a sample surface with a 22 keV Au^+ primary ion beam with 2 nA current in direct current (DC) mode for 5 min. Test experiments were carried out with blank ITO slides to evaluate the optimal sputtering time and to determine the m/z at which the FM were observable. The slides were washed in hexane and ethanol prior to the sputtering process. The FM were sputtered for 1, 3, 5, 10, 15, and 20 min. The sputtering time of 5 min was selected as optimal. In the further experiments with the tissue sections, the FM were implanted on the glass slide next to the tissue section and on the tissue section itself as shown in Figure 1. After the FM implantation, the tissue sections were imaged

with both techniques over the whole or selected area including the outside FM.

SIMS-MSI. Samples were analyzed using a TRIFT II (Physical Electronics, USA) time-of-flight secondary ion mass spectrometer (TOF-SIMS) equipped with a Au liquid ion metal gun, producing a 22 keV Au^+ primary ion beam. The sample bias was 3 kV. The spectra were calibrated on low mass fragments H, CH_3 , Na, and Au. The images were acquired in positive ion mode with a 128 μm raster size per tile resulting in a 500 nm pixel size or 162.5 μm raster size per tile resulting in 635 nm pixel size for rat brain and BC tissue, respectively. Acquisition and data analysis were performed by the WinCadence software package (Physical Electronics, USA).

MALDI-MSI. After the SIMS measurement, the samples were coated with a matrix solution (10 mg/mL α -cyano-4-hydroxycinnamic acid (CHCA) in 70% methanol solution with 0.2% TFA) using a vibrational sprayer (ImagePrep, Bruker, Germany). Samples were analyzed on the MALDI-Q-TOF instrument (Synapt HDMS, Waters, UK) in positive ion mode in the mass range of $m/z = 0-1000$ Da. Poly(ethylene glycol) (PEG) was used as an external standard for instrument calibration. The images were acquired with a raster step size of 100 and 150 μm for brain and BC tissue, respectively. The data was analyzed using the BioMap software (Novartis, Switzerland).

Note that it is imperative to perform the SIMS analysis prior to the MALDI measurements due to the discrepancy in surface damage between the two techniques. MALDI removes more surface material per pixel compared to SIMS that is minimally invasive.

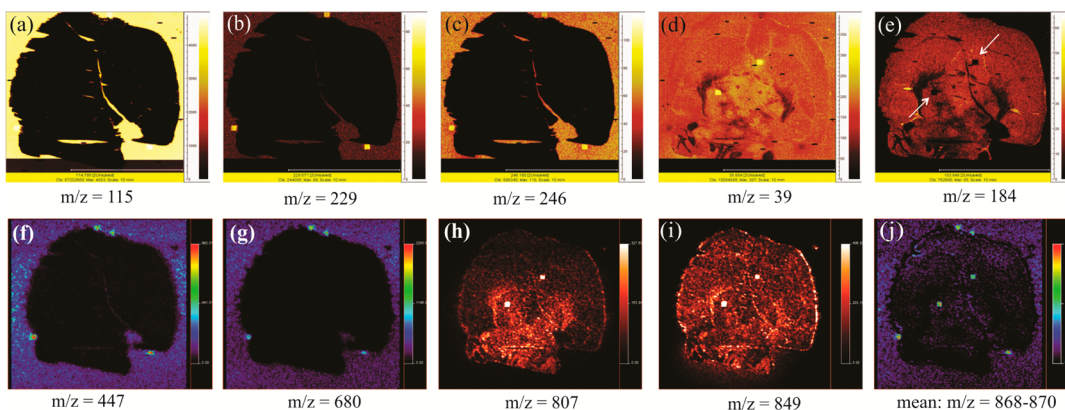


Figure 3. Brain tissue section. High spatial resolution SIMS images (a–e). Off-tissue FM: (a) m/z 115 (indium), (b) m/z 229 (In_2^+), and (c) m/z 246 (In_2O^+); on-tissue FM: (d) m/z 39 (potassium) and (e) m/z 184 (PC headgroup). Square signal depleted areas are indicated by white arrows. MALDI-MSI images of FM (f–j). Adjacent to the tissue section: (f) m/z 447 and (g) m/z 680; on-tissue FM: (h) m/z 807 and (i) m/z 849. (j) Off- and on-tissue FM within the mass window of 868–870 Da.

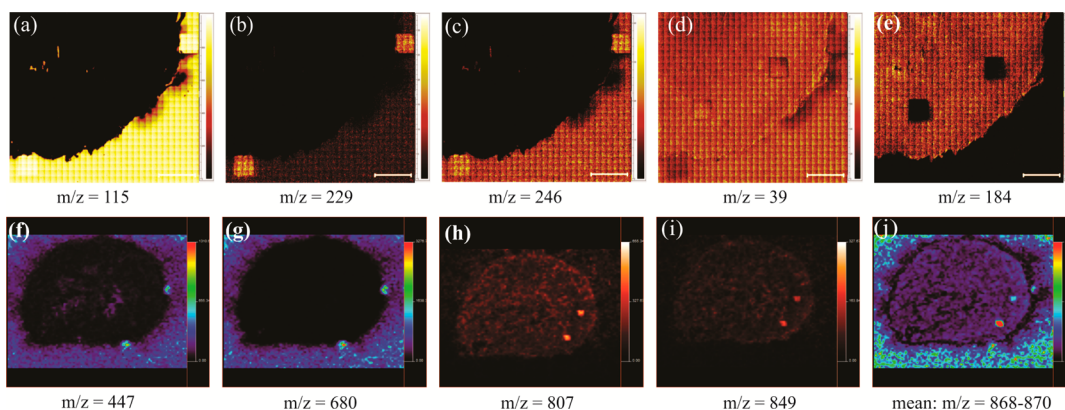


Figure 4. Breast cancer tissue. High spatial resolution SIMS images of the selected area (a–e). Off-tissue FM: (a) m/z 115 (indium), (b) m/z 229 (In_2^+), and (c) m/z 246 (In_2O^+); on-tissue FM: (d) m/z 39 (potassium) and (e) m/z 184 (PC headgroup). MALDI images of FM on the entire tissue section (f–j). Adjacent to the tissue section: (f) m/z 447 and (g) m/z 680; on-tissue FM: (h) m/z 807 and (i) m/z 849. (j) Off- and on-tissue FM within the mass window of m/z 868–870.

Principal Component Analysis. Principal component analysis (PCA) was performed on the blank ITO slide data sets to further evaluate the m/z characteristic for the off-tissue FM. For PCA, our in-house developed ChemomeTricks toolbox for MATLAB was used. Results of PCA on SIMS and MALDI measurements of the blank ITO slides are included in the Supporting Information (Figures S1 and S2).

RESULTS AND DISCUSSION

SIMS Measurements of the FM on a Blank ITO Slide.

We performed test measurements of the sputtered FM implanted on a blank ITO slide in order to select the optimal sputtering time and to determine the peaks related to the off-tissue FM. Peaks related to the ITO layer of the glass slides showed correlation with the sputtered areas as shown in Figure 2. Peaks at m/z 115 (In), 229 (In_2^+), and 246 (In_2O^+) showed higher intensity within the FM fields. The peak at m/z 39 corresponding to potassium was depleted at the FM fields as a result of the DC sputtering procedure. PCA revealed other peaks characteristic for the FM area (see Supporting Information Figure S1). Five min sputtering time was selected as optimal when sufficient visibility of the FM at all determined m/z was obtained. Longer sputtering periods resulted in distorted FM shapes.

MALDI-MSI Measurements of the Off-Tissue FM on a Blank ITO Slide. After the deposition of the FM, the marked blank ITO slide was covered with matrix and MALDI imaged. Figure 2b shows a spectral comparison of a region of interest within 5 min sputtered FM (in red) and within a matrix-only area (in blue). (Note the regions of interest were of the same size.) The peaks related to the FM are marked with arrows and annotated with the respective m/z values. Figure 2c shows images of the selected FM-related peaks. Results of PCA confirmed these m/z as being correlated with the FM areas as shown in the Supporting Information (Figure S2).

SIMS and MALDI Measurements of FM on Tissue Samples. Off- and on-tissue FM were sputtered next to and on top of the tissue samples as described in the Experimental Section. The tissue sections were subsequently imaged using SIMS and MALDI. Figures 3 and 4 show some of the off- and on-tissue FM on brain and BC tissue, respectively. The off-tissue FM are in correlation with the blank ITO slide measurements. Imaged with SIMS, they are clearly visible at m/z 115 (In^+), 229 (In_2^+), and 246 (In_2O^+) as shown in Figures 3a–c and 4a–c. Measured with MALDI, all m/z found during the blank ITO slide measurements were also visible. For illustration, m/z 447 and 680 are shown in Figures 3f,g and 4f,g.

The on-tissue FM were observed in the SIMS data set with a high intensity at m/z 39 (Figures 3d and 4d) and as squares

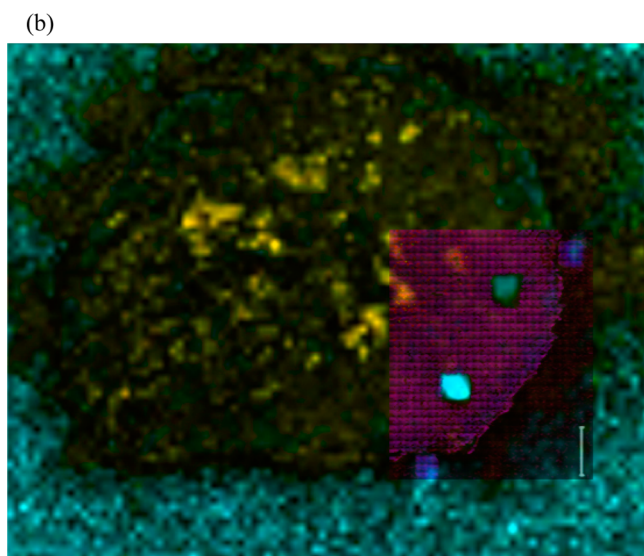
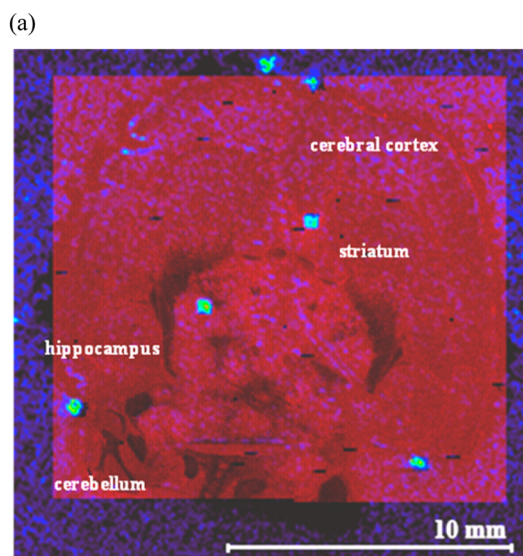


Figure 5. Manually coregistered overlay of (a) MALDI image (back) with 4 FM shown within the mass window m/z 868–870 in green and the SIMS overlaid images of In_2^+ (m/z 229) and potassium (m/z 39) in red (front). (b) MALDI image of the whole tissue section (back) with 4 FM shown within the mass window m/z 868–870 and m/z 490 and the SIMS overlaid image of the selected region of In_2^+ (m/z 229) and PC (m/z 184).

depleted in the signal at m/z 184 (Figures 3e and 4e). This indicates that the on-tissue FM are potassium rich and phosphocholine (PC) depleted and are likely related to the tissue surface alterations as a result of the DC sputtering procedure. Within the MALDI data sets, the on-tissue FM were displayed in all MS images of m/z higher than 500 Da. The individual species likely correspond to various gold clusters. Most importantly, they are created independent of the tissue type. Images of the selected m/z values are shown in Figures 3h,i and 4h,i. Figures 3j and 4j show both types of FM in the same image. Such an image can be constructed by selecting a broader mass window within the BioMap software. The selected mass window is shown below the images. Spectral comparison of MALDI on- and off-tissue FM is shown in the Supporting Information (Figure S3). The Supporting Informa-

tion also contains a table which summarizes m/z typical for off- and on-tissue FM observed by both modalities (see Supporting Information Table S1).

A demonstration of the easy coregistration using the SIMS generated fiducial markers is provided in Figure 5. Figure 5a shows a manual multimodal overlay of a SIMS and a MALDI FM image. The SIMS generated In_2^+ (m/z 229) and potassium (m/z 39) images from Figure 3b,d were overlaid in order to display the squares where the FM have been created. The MALDI image of the mass window m/z 868–879 from Figure 3h shows the FM with lower spatial resolution. The FM visible by both modalities can now be aligned during the coregistration procedure. Subsequently, all MALDI and SIMS images extracted from these two experiments can be overlaid as now all the coregistration coordinates are known. The MALDI FM images are not aligned with all SIMS FM completely due to the nature of matrix crystallization and lower spatial resolution of MALDI measurements. The described workflow can also be applied on selected parts of the tissue samples. This might be especially useful when examining regions of interest with high spatial resolution. For example, a coregistration of the selected high-resolution SIMS images at m/z 184 and 229 from Figure 4b,e can be overlaid with the MALDI image of the whole BC tissue section as shown in Figure 5b. The MALDI image for the coregistration consists of an overlay of the distribution of m/z = 490 and the image of the mass window 868–879 from Figure 4j with all observed FM.

CONCLUSION

Multimodal imaging requires appropriate coregistration of different images in order to obtain unique complementary information about the structure and composition of tissue sections. This Technical Note describes a clean and simple way to generate FM both on-tissue and off-tissue by means of a primary ion beam from the SIMS instrument. We have shown that the gold sputtered FM can be visualized by optical, SIMS, and MALDI imaging on a plain brain tissue sample as well as on a breast cancer tissue sample. We conclude that sputter generated fiducial markers are a suitable technique for MSI image coregistration.

ASSOCIATED CONTENT

Supporting Information

Results of principal component analysis of both MALDI and SIMS measurements of the blank ITO slide; spectrum and table of peaks related to the gold sputtered fiducial markers. This material is available free of charge via the Internet at <http://pubs.acs.org/>

AUTHOR INFORMATION

Corresponding Author

*Phone: +31-20-7547100. Fax: +31-20-7547290. E-mail: heeren@amolf.nl.

Author Contributions

[†]N.O.P. and K.S. contributed equally to this manuscript.

Notes

The authors declare no competing financial interest.

ACKNOWLEDGMENTS

The participation of N.O.P. in the work has been financed by the European 215 Union, European Social Fund. K.S. acknowledges financial support by the European Social Fund

and the FAFIS project funded by the Czech Republic under project no. CZ.1.07/2.2.00/28.0194. The authors acknowledge financial support from the dutch funding programs TA-COAST and COMMIT. This work is part of the research program of the Foundation for Fundamental Research on Matter (FOM), which is part of The Netherlands Organization for Scientific Research (NWO).

■ REFERENCES

- (1) Chughtai, K.; Heeren, R. M. A. *Chem. Rev.* **2010**, *110*, 3237–3277.
- (2) Pól, J.; Strohalm, M.; Havlíček, V.; Volný, M. *Histochem. Cell Biol.* **2010**, *134*, 423–443.
- (3) Passarelli, M. K.; Winograd, N. *Biochim. Biophys. Acta, Mol. Cell Biol. Lipids* **2011**, *1811*, 976–990.
- (4) Chughtai, S.; Chughtai, K.; Cillero-Pastor, B.; Kiss, A.; Agrawal, P.; MacAleese, L.; Heeren, R. M. A. *Int. J. Mass Spectrom.* **2012**, *325–327*, 150–160.
- (5) Walch, A.; Rausser, S.; Deininger, S.-O.; Hofler, H. *Histochem. Cell Biol.* **2008**, *130*, 421–434.
- (6) Sjövall, P.; Lausmaa, J.; Johansson, B. *Anal. Chem.* **2004**, *76*, 4271–4278.
- (7) Fuoco, E. R.; Gillen, G.; Wijesundara, M. B. J.; Wallace, W. E.; Hanley, L. J. *Phys. Chem. B* **2001**, *105*, 3950–3956.
- (8) Sheraz née Rabbani, S.; Barber, A.; Fletcher, J. S.; Lockyer, N. P.; Vickerman, J. C. *Anal. Chem.* **2013**, *85*, 5654–5658.
- (9) Todd, P. J.; Schaaff, T. G.; Chaurand, P.; Caprioli, R. M. *J. Mass Spectrom.* **2001**, *36*, 355–369.
- (10) Brunelle, A.; Touboul, D.; Laprévotte, O. *J. Mass Spectrom.* **2005**, *40*, 985–999.
- (11) van Hove, E. R. A.; Blackwell, T. R.; Klinkert, I.; Eijkel, G. B.; Heeren, R. M. A.; Glunde, K. *Cancer Res.* **2010**, *70*, 9012–9021.
- (12) Murphy, R. C.; Hankin, J. A.; Barkley, R. M.; Zemski Berry, K. A. *Biochim. Biophys. Acta, Mol. Cell Biol. Lipids* **2011**, *1811*, 970–975.
- (13) Goto-Inoue, N.; Hayasaka, T.; Zaima, N.; Setou, M. *Biochim. Biophys. Acta, Mol. Cell Biol. Lipids* **2011**, *1811*, 961–969.
- (14) Chughtai, K.; Jiang, L.; Greenwood, T. R.; Klinkert, I.; Amstalden van Hove, E. R.; Heeren, R. M. A.; Glunde, K. *Anal. Chem.* **2012**, *84*, 1817–1823.
- (15) Parker, C. C.; Damyanovich, A.; Haycocks, T.; Haider, M.; Bayley, A.; Catton, C. N. *Radiother. Oncol.* **2003**, *66*, 217–224.
- (16) Unlu, M. Z.; Krol, A.; Magri, A.; Mandel, J. A.; Lee, W.; Baum, K. G.; Lipson, E. D.; Coman, I. L.; Feiglin, D. H. *Comput. Biol. Med.* **2010**, *40*, 37–53.
- (17) Lim, Y. K.; Kwak, J.; Kim, D. W.; Shin, D.; Yoon, M.; Park, S.; Kim, J. S.; Ahn, S. H.; Shin, J.; Lee, S. B.; Park, S. Y.; Pyo, H. R.; Kim, D. Y.; Cho, K. H. *Int. J. Radiat. Oncol.* **2009**, *74*, 1609–1616.